Spectrochimica Acta Part A: Molecular and Biomolecular Spectroscopy 240 (2020) 118601

Contents lists available at ScienceDirect

Spectrochimica Acta Part A: Molecular and Biomolecular Spectroscopy

journal homepage: www.elsevier.com/locate/saa

Fluorescence properties and quantum-chemical modeling of *tert*-butyl-substituted porphyrazines: Structural and ionization effect

O.A. Dmitrieva [a], Yu.B. Ivanova [a], A.S. Semeikin [b], N.Z. Mamardashvili [a,*]

[a] G. A. Krestov Institute of Solution Chemistry of the Russian Academy of Sciences, Akademicheskaya st., 1, Ivanovo, Russia
[b] Ivanovo State University of Chemistry and Technology, Sheremetevsky av., 7, Ivanovo, Russia

ARTICLE INFO

Article history:
Received 27 February 2020
Received in revised form 13 May 2020
Accepted 8 June 2020
Available online 15 June 2020

Keywords:
Porphyrazines
Acidic and fluorescence properties
Energy levels
The highest occupied and the lowest unoccupied molecular orbitals

ABSTRACT

Synthesis and identification of tetrakis-[5,6-bis(4-*tert*-butylphenyl)pyrazino] porphyrazine, tetra-(4-*tert*-butyl) phthalocyanine and octakis-(4-*tert*-butylphenyl)porphyrazine were carried out. Spectrophotometric method was used to study the spectral, acidic and fluorescence properties of the synthesized compounds. It was determined that the synthesized *tert*-butyl-substituted porphyrazines exhibit a high sensitivity of fluorescence to the molecule ionization. To understand the features of the spectral properties the geometry optimization and an analysis of energy levels and localization of highest occupied and lowest unoccupied molecular orbitals of the studied compounds were performed on the basis of density functional theory with the BP86 functional and the def2-TZVP basis set. The effect of substituents in molecular fragments of the macrocycle on the acidic and electro-optical properties of the studied compounds is revealed. Materials with pH-tunable fluorescence were designed.

1. Introduction

Porphyrazines, as an important class of porphyrinoid macrocycles, carrying pyrazine rings directly annulated to the pyrrole rings of the porphyrazine core, have been presented in recent years as photoactive materials with clear advantages over the porphyrins [1–3]. An area of further expansion of new porphyrazines macrocycles can be directed to the synthesis of new phthalocyanines-like macrocycles opening a route to new forms of investigation and promising potential practical applications [4,5]. It should be noted that all porphyrazines reveal amphoteric properties [6]. Tetrazaporphyrins are able to protonate along the *meso*-nitrogen atoms of the macrocycle in acidic media and deprotonate along the intracyclic N-H groups in high basic media. Phthalocyanines are protonated along bridging nitrogen atoms of the macrocycle upon interaction with strong acids (concentrated sulfuric and chlorosulfonic acids) up to the formation of tetraprotonated salts and are deprotonated in media of strong bases (hydrogens of the pyrrole NH groups can be cleaved with formation of corresponding tetrapyrrolic dianions). Porphyrazines, as structural analogues of porphyrins, are widely used as effective catalysts for oxidation-reduction reactions, in the production of light-resistant green and blue dyes and pigments, as well as optical materials for laser technologies [7,8]. Based on the foregoing, the studies of porphyrazines have great potential for practical use and are in demand and relevant.

In this work, we synthesized tetrakis[5,6-bis(4-*tert*-butylphenyl) pyrazino]porphyrazine, tetra(4-*tert*-butyl)phthalocyanine and octakis (4-*tert*-butylphenyl)porphyrazine. The spectrophotometric method was used to study their spectral, acidic and fluorescence properties. In order to establish the effect of the molecule ionization on the of fluorescence quenching mechanism the geometry optimization, an analysis of energy levels and localization of highest occupied and lowest unoccupied molecular orbitals of the synthesized porphyrazines were performed on the basis of density functional theory (DFT) with the BP86 functional and the def 2-TZVP basis set. The significant influence of substituent nature and its position in the macrocycle on the acidic and fluorescence properties of the synthesized porphyrazines is revealed.

2. Experimental part

2.1. Tetrakis[5,6-bis(4-tert-butylphenyl)pyrazino]porphyrazine (I)

50 mg of lithium (7.2 mmol) was dissolved in 10.0 ml of ethylene glycol under heating. Then 450.0 mg of 2,3-dicyano-5,6-bis(4-*tert*-butylphenyl)pyrazine (3.56 mmol) was added to the solution and resulting mixture was refluxing for 3 h and cooled. The precipitate was filtered off, washed with water and dried at 70 °C in air. The residue was dissolved in chloroform, acidified with trifluoroacetic acid until the color turned bluish to green and chromatographed on silica gel eluting with chloroform. The filtrate was evaporated, porphyrazine was precipitated with methanol, filtered and dried at 70 °C in air. Yield: 70.0 mg (17.5%). R_f (Silufol): 0.85 (benzene-methanol, 30:1). MALDI-TOF (*m*/

* Corresponding author at: Akademicheskaya Str.1, 153045 Ivanovo, Russia.
E-mail address: ngm@isc-ras.ru (N.Z. Mamardashvili).

https://doi.org/10.1016/j.saa.2020.118601
1386-1425/

z), Found 1582.926 $[M+2H]^+$, Calculated 1580.901. ^{1}H NMR ($CDCl_3$) δ, ppm: 8.05 d (16H, $J = 8.1$ Hz, 2,6-H-Ar); 7.58 d (16H, $J = 8.1$ Hz, 3,5-H-Ar); 1,48 s (72H, H-tBu); −0.66 s (2H, NH). UV–Vis spectra of the **I**, λ_{max}, nm (lg ε): 679 (5.28), 648 (5.18), 473 (4.83), sh, 372 (5.15) (chloroform); 464sh (4.55), 593sh (4.38), 616sh (4.48), 646 (4.97), 674 (5.07) (acetonitrile). UV–Vis spectra of the $(I)^{2-}$, λ_{max}, nm (lg ε): 665 (4.97), 603sh (4.29) (acetonitrile+DBU).

2,3-Dicyano-5,6-bis(4-tert-butylphenyl)pyrazine. A solution of 4.0 g (12.4 mmol) bis(4-*tert*-butylphenyl)ethanedione, 1.4 g (13.0 mmol) of diaminomaleodinitrile and 100 mg of *p*-toluenesulfonic acid in 15.0 ml of methanol was refluxing for 3 h, then the mixture was cooled. The precipitate was filtered off, washed with methanol and dried in air at room temperature. Yield 4.2 g (85.9%). Melting point: 161–165 °C. MALDI-TOF (*m/z*), Found 395.667 $[M+H]^+$, Calculated 395.53. ^{1}H NMR ($CDCl_3$) δ, ppm: 7.55 dt (4H, $J = 8.6$ Hz, $^1J = 2.1$ Hz; 2,6-H-Ar); 7.41 dt (4H, $J = 8.6$ Hz, $^1J = 2.1$ Hz; 3,5-H-Ar); 1.35 s (18H, H-tBu).

2.2. Tetra(4-tert-butyl)phthalocyanine (II)

The mixture of 3.0 g 4-*tert*-butylphthalonitrile (16.3 mmol), 0.12 g of lithium (17.1 mmol) and 20.0 ml of dried quinoline (as a solvent) were refluxing for 3 h, cooled and then concentrated hydrochloric acid (30.0 ml) and water (150.0 ml) were added to the mixture with stirring. The precipitate was filtered off, washed with water and dried. The residue was dissolved in chloroform and chromatographed on alumina of the III degree of activity with chloroform as eluent. The eluate was evaporated, the product was precipitated with methanol, filtered off, washed with methanol and dried at 70 °C in air. Yield: 0.80 g (36.2%). R_f (Silufol): 0.52 (chloroform - hexane, 3:1). MALDI-TOF (*m/z*), Found 739.156 $[M]^+$, Calculated 738.981. ^{1}H NMR ($CHCl_3$) δ, ppm: 9.16 m (4H, 6-H); 8.86 m (4H, 3-H); 8.15 m (4H, 5-H); 1.90 m (36H, H-tBu); −2.60 bs (2H, NH) ($CDCl_3$) (mixture of atropisomers). UV–Vis spectra of the II, λ_{max}, nm (lg ε): 701 (5.10), 664 (5.03), 645 (4.59), 603 (4.41), 342 (4.81) (chloroform); 599 (4.21), 638_{sh} (4.36), 661 (4.77), 696 (4.82) (acetonitrile). UV–Vis spectra of the $(II)^{2-}$, λ_{max}, nm (lgε): 400 (4.75), 608_{sh} (4.19), 673 (4.75) (acetonitrile + DBU).

2.3. Octakis(4-tert-butylphenyl)porphyrazine (III)

A solution of 0.20 g Pb-octakis(4-*tert*-butylphenyl)porphyrazine (0.13 mmol) in trifluoroacetic acid (5.0 ml) was refluxing in argon atmosphere for 1 h, then it was poured into water and concentrated ammonia solution (5.0 ml) was added to the resulting mixture. The precipitate was filtered off, washed with water and dried. The product was dissolved in chloroform and chromatographed on silica gel with chloroform as eluent. The eluate was evaporated to a minimal amount and diluted with methanol (25.0 ml). Precipitated residue was filtered off, washed with methanol and dried in air at 70 °C. Yield: 120.0 mg (67.3%). R_f (Silufol): 0.81 (benzene-hexane, 1: 1). MALDI-TOF (*m/z*), Found 1372,825 $[M+H]^+$, Calculated 1371,950. ^{1}H NMR ($CHCl_3$) δ, ppm: 7.81 d (2H, $J = 8.1$ Hz, 2,6-H-Ar); 7.56 d (2H, $J = 8.1$ Hz, 3,5-H-Ar); 1.39 s (72H, tBu); 0,10 bs (2H, NH). UV–Vis spectra of the III: λ_{max}, nm (lg ε): 677 (4.60), 610 (4.46), 484 (4.43), 376 (4.63) (chloroform); 712 (4.92), 674 (4.99), 612 (4.78), 473 (4.88), 402_{sh} (4.79), 378 (4.91) (acetonitrile). UV–Vis spectra of the $(III)^{2-}$: ($\lambda_{max,}$ nm (lg ε): 672 (5.03), 614_{sh} (4.88), 468 (4.76), 372_{sh} (4.89), 321_{sh} (4.99) (acetonitrile + DBU).

Pb(II)-2,3,7,8,12,13,17,18-octakis(4-tert-butylphenyl)porphyrazine. A mixture of 0.50 g 1,2-bis(4-*tert*-butylphenyl)fumaronitrile (1.46 mmol) and 0.3 g lead acetylacetonate (0.74 mmol) was refluxing in ethyleneglycol (20.0 ml) for 2 h. Then the mixture was cooled, the precipitate was filtered off, washed with water and dried in air at 70 °C. The product was dissolved in methylene chloride and chromatographed on silica gel, eluting with methylene chloride. The eluate was evaporated to a minimal amount and diluted with methanol (25.0 ml). Precipitated residue was filtered off, washed with methanol and dried in air at 70 °C. Yield: 140.0 mg (24.3%). MALDI-TOF (*m/z*), Found 1578.393 $[M+H]^+$, Calculated 1577.141. ^{1}H NMR ($CDCl_3$) δ, ppm: 8.37 d (16H, $J = 8.3$ Hz, 2,6-H-Ar); 7.65 d (16H, $J = 8.3$ Hz, 3,5-H-Ar); 1.54 s (72H, H-tBu) ($CDCl_3$). UV–Vis λ_{max}, nm (lg ε): 677 (4,95); 423 (4,84) ($CHCl_3$).

Bis(4-tert-butylphenyl)fumaronitrile. 4.6 g of sodium (0.2 mol) was dissolved in methanol (75.0 ml) with stirring, and resulting solution was gradually added while cooling (temperature below 10 °C) to a stirring solution of 25.4 g iodine (0.1 mol) and 17.3 g (4-*tert*-butylphenyl) acetonitrile (0.1 mol) in a mixture of methanol (70.0 ml) and ether (375 ml). The reaction mixture was stirred for 30 min and washed 3 times with water, then evaporated to a half and cooled overnight in the refrigerator. The precipitate was filtered off, washed with a little amount of ether and dried. Yield: 6.20 g (36.3%). Melting point: 222–224 °C. MALDI-TOF (*m/z*), Found 343.460 $[M+H]^+$, Calculated 343.49. ^{1}H NMR ($CDCl_3$) δ, ppm: 7.81 dt (4H, $J = 8.5$ Hz, $^1J = 2.0$ Hz, 2,6-H-Ar); 7.56 dt (4H, $J = 8.5$ Hz, $^1J = 2.0$ Hz, 3,5-H-Ar); 1.37 s (18H, H-tBu).

The individuality of the compounds was controlled by TLC on Silufol plates with a layer thickness of 0.5 mm (Merck), eluent: chloroform. The purification and identification of the compound were carried out according to [9]. Spectrophotometric titration with acetonitrile solutions of perchloric acid in acetonitrile was carried out on Cary 100 spectrophotometers from Varian and SPEC SSP-715. A highly purified acetonitrile was used as dipolar aprotic solvent (water content was <0.03%), in which the initial objects were in molecular form, that was confirmed by the initial spectra of porphyrins. The experimental procedure, preparative chemistry, and experimental data processing are presented in detail in [10–12]. Proton magnetic resonance spectra (^{1}H NMR) were measured on a Bruker AV III-500 spectrophotometer (internal standard - TMS). Mass spectra were recorded on a Shimadzu Axima Confidence time-of-flight mass spectrometer (MALDI-TOF).

Fluorescence properties of the free ligands (I-III) in acetonitrile and their ionic forms (I^{2-}, II^{2-} and III^{2-}) in a mixture of acetonitrile-DBU were studied at 295 K. Fluorimetric measurements of solutions of porphyrazines were carried out on a Shimadzu RF-5301 fluorimeter. Fluorescence was measured for highly dilute solutions (<10^{-7} mol/l) due to possible strong reabsorption processes observed at high concentrations of solutions, which can often provoke a bathochromic shift of fluorescence maxima for some phthalocyanines [13].

The fluorescence spectra of the studied samples in toluene were compared with standard values from literature. The Zinc-phthalocyanine (ZnPc) was chosen as the standard, for which the quantum yield in pyridine is known and equals to 0.3 [14]. The corresponding integral fluorescence intensities were calculated. The quantum fluorescence yield of compounds (I-III) and their ionic forms (I^{2-}, II^{2-}, III^{2-}) was calculated by the standard method [15] using a PFPC software package v.2.04 according to formula (1):

$$Q_x = Q_{st}\frac{I_x A_{st} n_x^2}{I_{st} A_x n_{st}^2} \quad (1)$$

where Q_x and Q_{st} are the quantum yields of the test sample and standard, respectively; A_x and A_{st} are their optical density at the excitation wavelength; I_x and I_{st} are the integrated intensities; n_x and n_{st} are the refractive indices of the solvents for the sample and standard, respectively. The error of the fluorimetric measurements was ~10%.

The calculations were carried out in the GAMESS v.12 software package [16]. The BP86 functional [17,18] and the base set def2-TZVP [19] was used for calculations. The BP86 functional provides high-precision calculations of the geometry of tetrapyrrole macrocycles. In some cases, this accuracy exceeds the accuracy provided by the frequently used B3LYP method [20–23]. A complete optimization of geometry of the free ligands (I-III) structures and their deprotonated forms (I^{2-}, II^{2-} and III^{2-}) were optimized in the ground state by DFT method. The results of theoretical calculation of energy levels and the

localization of the highest occupied molecular orbital (HOMO) and the lowest free molecular orbital (LUMO) of compounds (I-III) calculated by the TD-DFT method. The calculations were performed in acetonitrile using the PCM solvation model [24–26]. The resulting structures were confirmed by the presence of minima on potential energy surfaces and the absence of imaginary vibration frequencies.

3. Results and discussion

3.1. Synthesis and acidic properties of porphyrazines

Tetrakis[5,6-bis(4-*tert*-butylphenyl)pyrazino]porphyrazine (I) was synthesized by a modified method [27] according with the Scheme 1. 2,3-dicyano-5,6-bis(4-*tert*-butylphenyl)pyrazine was obtained by condensation of 1,2-bis(4-*tert*-butylphenyl)ethanedione with diaminomaleinodinitrile in methanol with the addition of catalytic amounts of *p*-toluenesulfonic acid. The cyclotetramerization of the *tert*-butylsubstituted pyrazine with a solution of lithium in ethylene glycol gave the target porphyrazine (I).

Tetra (4-*tert*-butyl)phthalocyanine (II) was prepared by a modified method [28] by cyclotetramerisation of 4-*tert*-butylphthalonitrile with lithium in boiling quinoline (Scheme 2).

Octakis-(4-*tert*-butylphenyl)porphyrazine was synthesized according by a modified method [29] with the Scheme 3. Bis(4-*tert*-butylphenyl)fumaronitrile was obtained by reaction of 4-*tert*-butylphenylacetonitrile with iodine in the presence of sodium methylate. The cyclotetramerisation of this compound in the presence of lead acetylacetonate in ethylene glycol gave Pb-octakis-(4-*tert*-butylphenyl) porphyrazine, demetallation of which resulted in the formation of corresponding porphyrazine-ligand (III) upon treatment with trifluoroacetic acid.

The synthesized compounds (I-III) were identified by UV–Vis, ^{1}H NMR and mass spectrometry and correspond to the data of [27–29]. The synthesis is described in detail in the experimental part.

The deprotonation of the porphyrins and porphyrazines (H_2P) and its derivatives on intracyclic nitrogen atoms in organic solvents in the presence of bases proceeds according to processes (Eqs. (2), (3)) [30]. The literature data for amyloxyl- and thiodiazole-derivatives of the phthalocyanine also indicate the implementation of these processes in DMSO medium [30].

$$H_2P \overset{k_{a1}}{\rightleftarrows} HP^- + H^+ \quad (2)$$

$$HP^- \overset{k_{a2}}{\rightleftarrows} P^{2-} + H^+, \quad (3)$$

where H_2P, HP^- and P^{2-} are molecular, mono- and double-deprotonated forms of the porphyrin ligand.

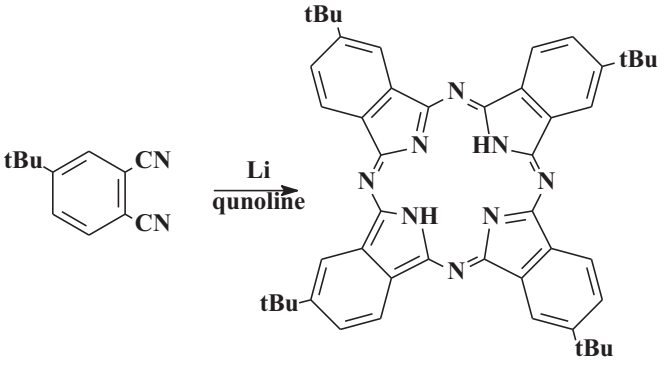

Scheme 2. Synthesis of the compound (**II**).

It should be mentioned that the study of acid properties of porphyrins and porphyrazines in DMSO is complicated by the fact that upon dissolution the ligand enters into an acid-base interaction with the electron-donating center of the DMSO molecule. This interaction is not accompanied by complete deprotonation of the tetrapyrrole macrocycle, and the mobility of protons of the NH groups noticeably increases, which manifests itself in a change of the UV–Vis spectra [31].

The titration of such a mixture requires additional components (organic acids) to adjust the concentrations of the forms in this mixture. In this case, the use of the acetonitrile (AN) -1,8-diazabicyclo[5.4.0]undec-7-ene (DBU) system (Eq. (4)) greatly facilitates this task, since the ligands in this solvent are in molecular form, which confirmed by UV–Vis spectra.

$$(\mathbf{I-III})-DBU-CH_3CN \quad (4)$$

The spectrophotometric titration of compounds (I-III) in the system (Eq. (4)) showed that with an increase in the DBU concentration two families of spectral curves were observed in the UV–Vis spectra of ligands, each of which corresponded to its own set of isosbestic points (Figs. 1–3). The presence of two families of isosbestic points in the UV–Vis spectra is characteristic of stepwise processes of the deprotonation [11]. The spectrophotometric titration of compounds (I-III) in the system (Eq. (4)) showed a change in the UV–Vis spectra in going from the molecular forms of the corresponding ligands to their double-deprotonated forms (Figs. 1–3). However, the spectrophotometric titration curves constructed on the basis of experimental data do not have pronounced steps (Figs. 1–3), which do not deny the staggering of ionization processes, but assume close values of the protonation constants for each reaction [32]. The extinction coefficients for

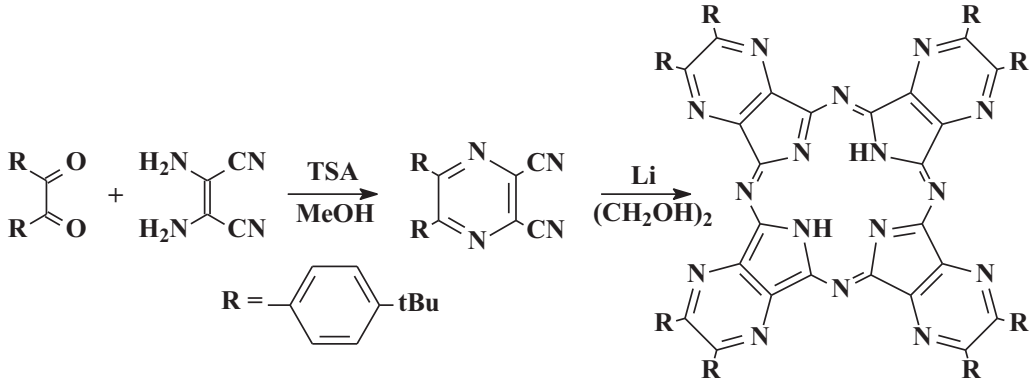

Scheme 1. Synthesis of the compound (**I**).

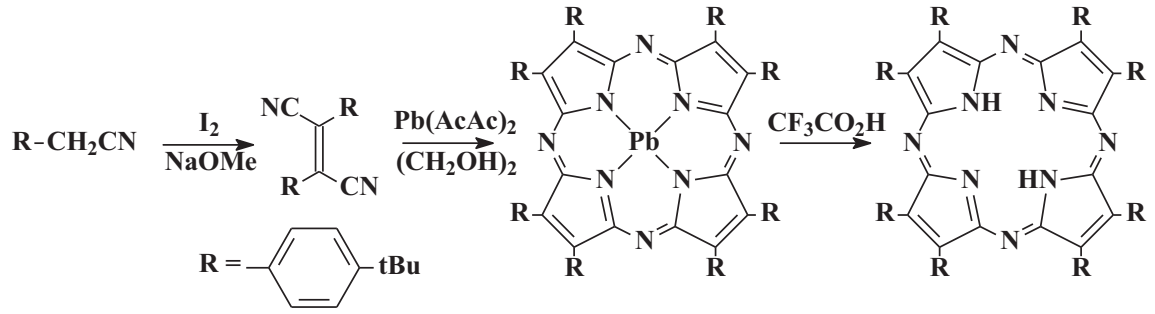

Scheme 3. Synthesis of the compound (**III**).

the forms of the studied compounds participating in the equilibriums (Eqs. (2), (3)) in the system (Eq. 4) were determined by the UV–Vis data and the total particle concentration of each ligand.

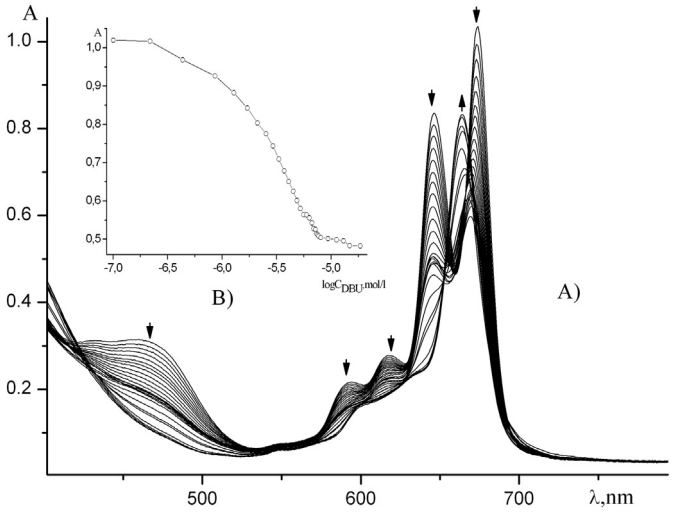

Fig. 1. UV–Vis spectra (A) and spectrophotometric titration curve (λ = 675 nm) (B) of the ligand (I) in the AN – DBU system, ($C_{porph.} = 8.78 \cdot 10^{-6}$ mol/l; $C_{DBU} = 0 \div 1.85 \cdot 10^{-5}$ mol/l), T = 298 K.

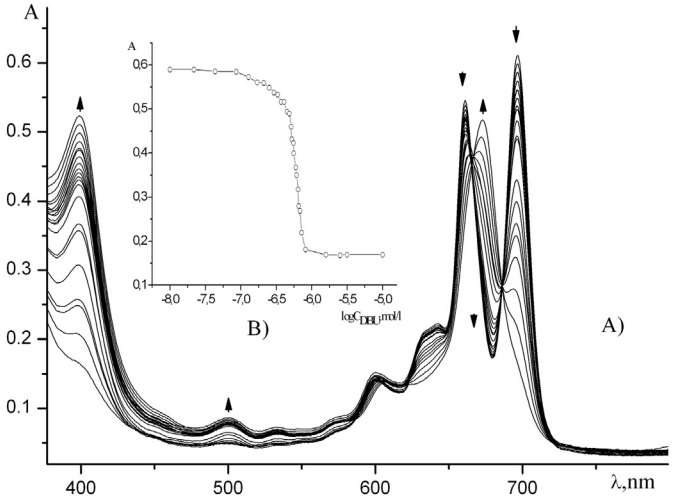

Fig. 2. UV–Vis spectra (A) and spectrophotometric titration curve (λ = 696 nm) (B) of the ligand (II) in the AN – DBU system, ($C_{porph.} = 0.92 \cdot 10^{-6}$ mol/l; $C_{DBU} = 0 \div 1.15 \cdot 10^{-5}$ mol/l), T = 298 K.

To calculate the total acidity constant, Eq. (5) was used:

$$pK_a = -\lg K_a = \lg(Ind) + n\lg c_{an} \quad (5)$$

where K_a - is the total acidity constant, c_{an} - is the analytical value of the DBU concentration in solution, *Ind* - is the indicator ratio P^{2-}/H_2P, n - is the number of dissociated protons (n = 2). The total acidity constants (pK_a) for the compounds (I-III) in the system (Eq. (4)) at 298 K were 11.11, 13.12 and 14.06, respectively. The error in the measurement of constants did not exceed 3–5%.

The nature of the substituent and its position in the macrocycle has a significant effect on the acidic properties of tetrapyrrole macrocycle. The studies have shown that the chemical modification of octakis(4-*tert*-butylphenyl)porphyrazine to tetra(4-*tert*-butyl)phthalocyanine and tetrakis[5,6-bis (4-*tert*-butylphenyl)pyrazino]porphyrazine leads to an increase in acidic constants of the compounds by one and three orders of magnitude, correspondingly. Phenyl and *tert*-butyl groups exhibit a rather weak +I-effect toward to the porphyrin system and contribute to a small violation of the planar structure of the macrocycle. Nitrogen atoms in the structures of the studied compounds can participate both in the redistribution of electron density over σ-bonds and in the π-π conjugation of the ligand macrocycle as a whole [33]. The remoteness of phenyl fragments with *tert*-butyl substituents in compound (I) from the reaction center and the presence of eight additional nitrogen atoms in condensed benzene rings probably make the prevail influence of nitrogen atoms on the electron density of intracyclic nitrogen atoms, which leads to a decrease in the strength of the NH-bond and contribute

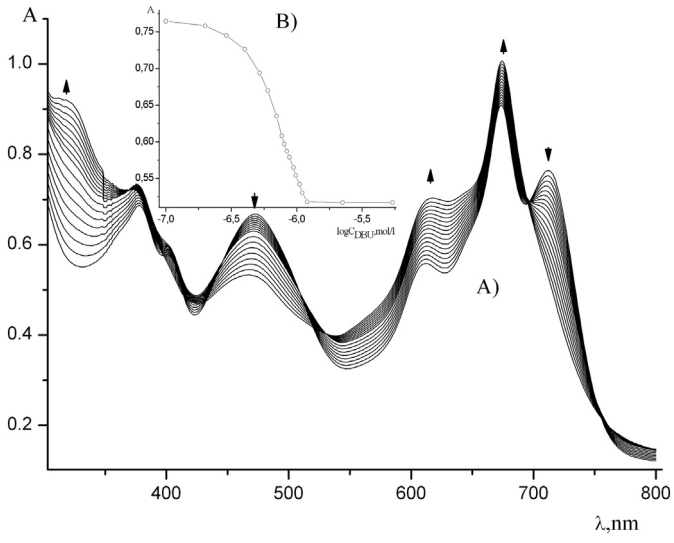

Fig. 3. UV–Vis spectra (A) and spectrophotometric titration curve (λ = 712 nm) (B) of the ligand (III) in the AN – DBU system, ($C_{porph.} = 0.90 \cdot 10^{-5}$ mol/l; $C_{DBU} = 0 \div 1.15 \cdot 10^{-5}$ mol/l), T = 298 K.

to a decrease in the effective stabilization of the formed anion. It is likely that reactivity change of the coordination center is the result of both the modification of the porphyrazine and phthalocyanine ligands, as well as the influence of peripheral substituents and the nature of the solvent.

3.2. Ground-state geometry

The calculated geometric parameters of the free ligands are presented in Fig. 4. The calculation results showed that the introduction of peripheral substituents in compounds (I) and (II) led to an increase in all bond lengths in macrocycles (Fig. 4). In the case of compound (III), a decrease in all bond lengths was observed except for C_1-C_2 and C1'-C2', which were extended by the introduction of phenyl substituents. The introduction of *tert*-butyl groups in compound (II) had an insignificant effect on the molecule geometry (the macrocycle did not change its flat structure) compared to unsubstituted phthalocyanine [23], while the complexity of the ligand structure of compound (I) led to an increase in the dihedral angles C_1-Np-C_1 and C_1'-NH-C_1' by 0.7 and 1.2°, respectively, compared with compound (II), resulting in steric twist that was formed during non-planar deformation of the macrocycle. The opposite effect was observed for compound (III). The angles C_1-Np-C_1 and C_1'-NH-C_1' decreased, leading to compression of the macrocycle. The deprotonation of ligands (I-III) leads to a slight increase in all bond lengths with the exception of C_1-Np and C_1-NH (Fig. 4), which is probably a consequence of the redistribution of

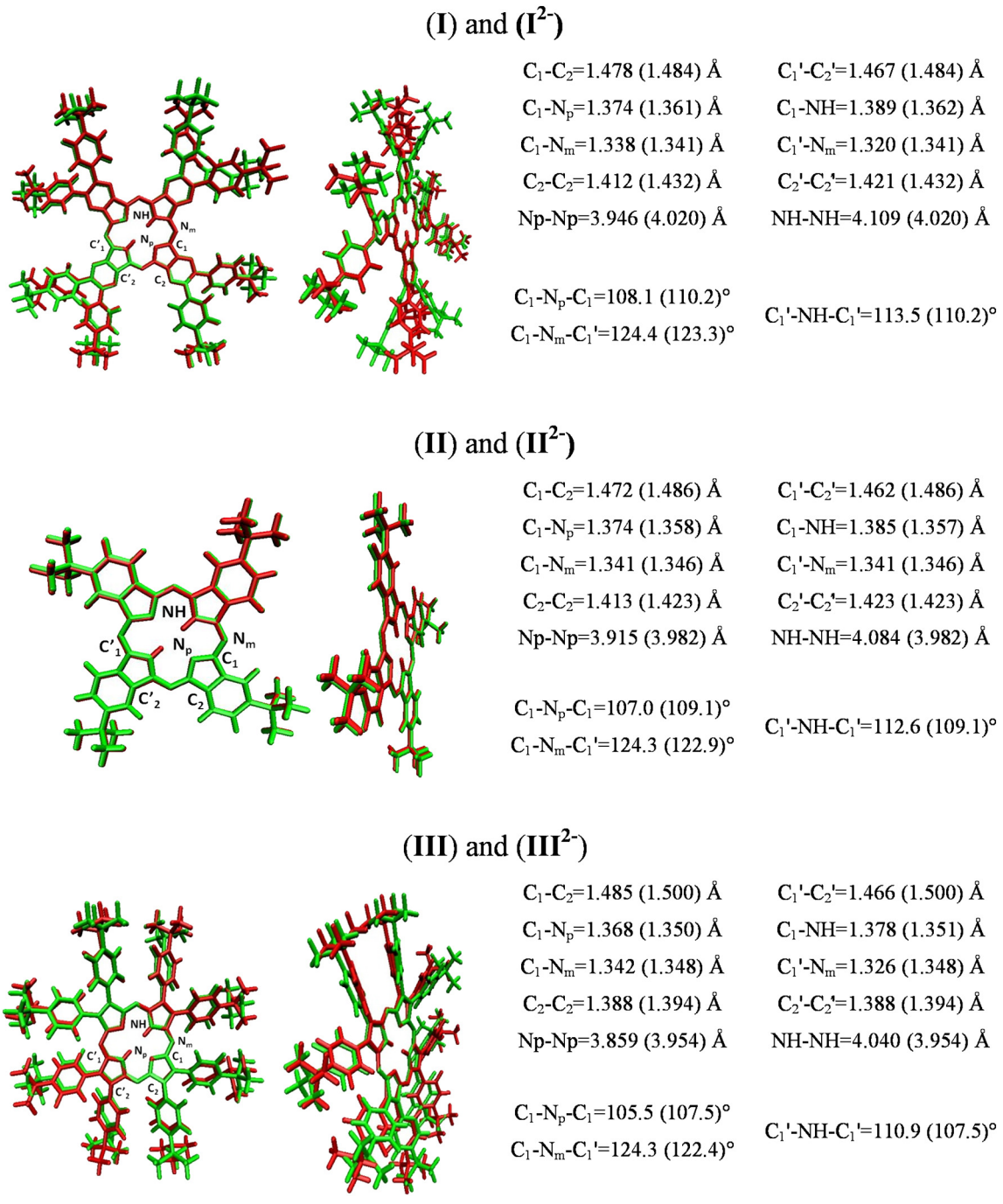

Fig. 4. Front and side views of the calculated structures and selected geometrical parameters for the compounds (I-III) (red color) and their deprotonated forms [$(I)^{2-}$ - $(III)^{2-}$] (green color).

electron density in intracyclic nitrogen atoms as a result of substituents influence on the σ-bonds.

To characterize non-planar distortions of the macrocycle of porphyrazines containing 24 atoms we introduced the quantity Δ24:

$$\Delta 24 = \sqrt{\frac{1}{24}\sum_{i=1}^{24}\Delta z_i^2} \quad (6)$$

where Δz_i is the deviation of the *i*-atom of the macrocycle from its middle plane.

An analysis of the calculated Δ24 values (Fig. 5) showed that the introduction of *tert*-butyl substituents into the condensed benzene rings of macrocycle (II) does not lead to non-planar distortions of the macrocycle in both molecular and ionic forms. The steric interaction arising between the phenyl substituents in compounds (I) and (III) leads to an out-of-plane ruffling deformation of the macrocycle (Fig. 5) for which the average deviation of carbon atoms is 0.02 Å (I) and 0.05 Å (III). The deprotonation of compounds (I) and (III) leads to a larger distortion of the ion structure (Fig. 5). It was found that for compound (I^{2-}) the average deviation of carbon atoms from the plane of the macrocycle increases to 0.1 Å and compound (III^{2-}) becomes characterized by a saddle-shaped macrocycle distortion with a mean carbon atom deviation of 0.5 Å (Fig. 5). Thus, the degree of non-planarity increases in the series II < I < III, which is consistent with the classical concepts of the stability of phthalocyanine structures in comparison with their azo-analogues.

3.3. Frontier molecular orbitals

The considered acidic properties of porphyrazines reflect the acidity of the medium according to Bronsted. Theories of acids and bases do not contradict, but complement each other and have a deep internal

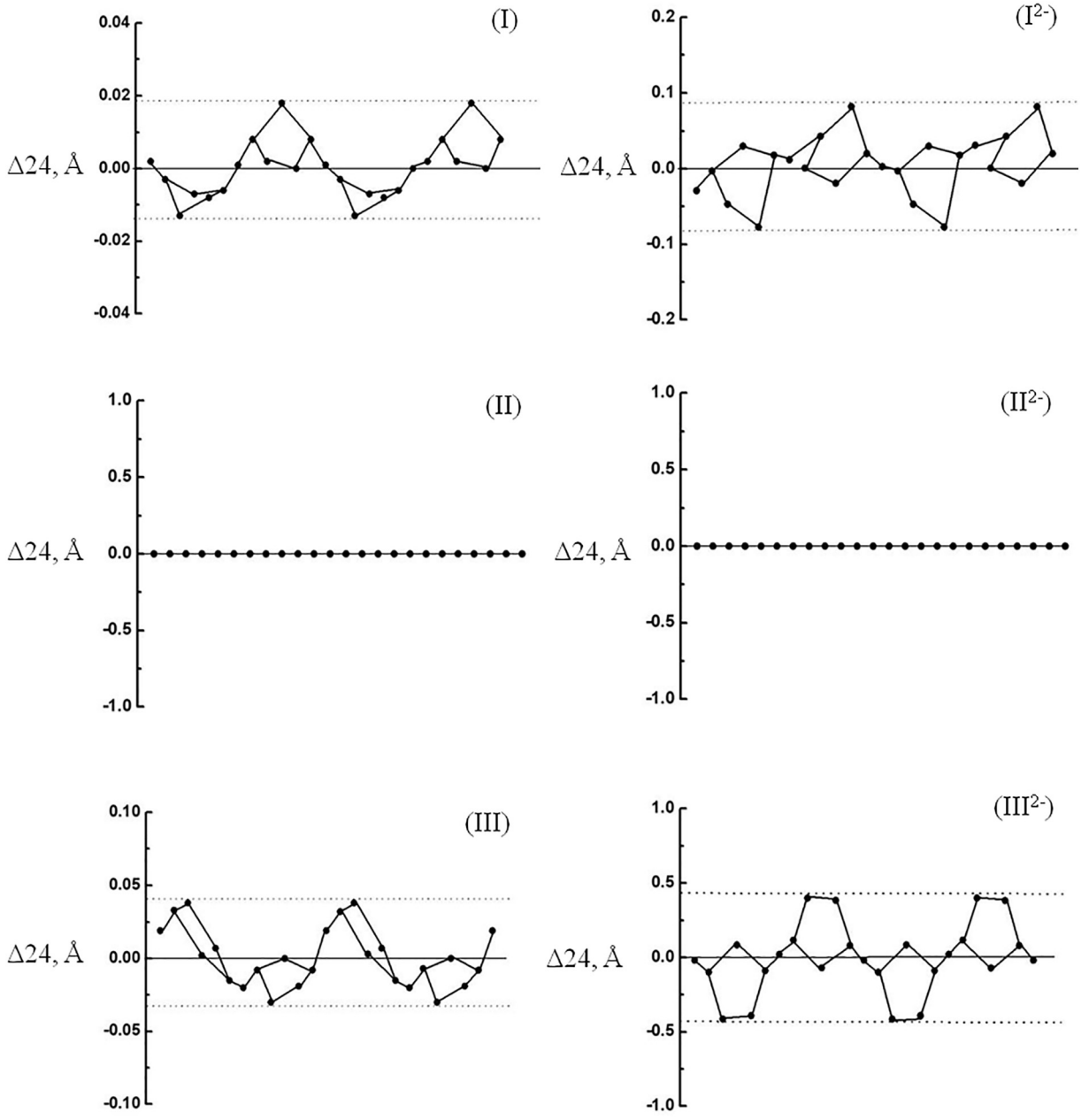

Fig. 5. View of the skeletal deviations of the 24 macrocycle atoms from their least-squares plane.

connection. So, acids, according to Bronsted, can be considered as a special case of Lewis acids, since the proton is characterized by a high affinity for the electron pair and can be considered, according to Luys, as an acid. Therefore, a theoretical calculation of the boundary molecular orbitals (MO) can provide information on the molecular reactivity and electron transfer ability, which usually occurs at the boundary of the system [34]. The states of the highest occupied molecular orbital (HOMO) and the lowest free molecular orbital (LUMO) are very important quantum parameters that play a role in the electrical and optical properties. In the redox reaction, the oxidizing agent has a low LUMO value, and the reducing agent has a high HOMO value. The nature of the substituent and its position in the macrocycle has a strong effect on the acidic properties of tetrapyrrole macrocycles. The results of theoretical calculation of energy levels and the localization of HOMO and LUMO of compounds (I-III) are presented in Fig. 6.

The comparison of the HUMO - LUMO energy gap of molecular orbitals (Fig. 5) shows that the presence of *tert*-butyl substituents in compound (II) leads to the smallest HOMO-LUMO gap, which is practically determined by the destabilization of HOMO compared to (I) and (III). The remoteness of aryl fragments from the reaction center of compound (I) leads to an increase in the energy gap and the stability of the HOMO orbital. In the case of compound (III), the influence of *tert*-butyl fragments through the phenyl buffer leads to slight destabilization of the HOMO and LUMO orbitals and, as a result, leads to an increase in the energy gap of HUMO - LUMO to 1.45 eV in comparison with compound (I). From the obtained MO values of HOMO and LUMO (Fig. 6), it follows that ligand (I) has the lowest LUMO value (−3.99 eV) and is a good oxidizing agent of all the porphyrazines presented. The electron-withdrawing ability of the compounds increases in the following order: (I) > (III) > (II).

3.4. Fluorescence emission spectroscopy

The fluorescence spectra and spectral-fluorescence characteristics are shown in Fig. 7 and Table 1. The data of the Table 1 and Fig. S1 indicate a low Stokes shift (several cm^{-1}) of the studied compounds (I) and (II), which is characteristic of a significant overlap of the absorption spectra with fluorescence spectra [35]. This is probably due to a slight relaxation of the molecule geometry, which occurs in the first excited state. However, a larger Stokes shift is observed in the case of compound

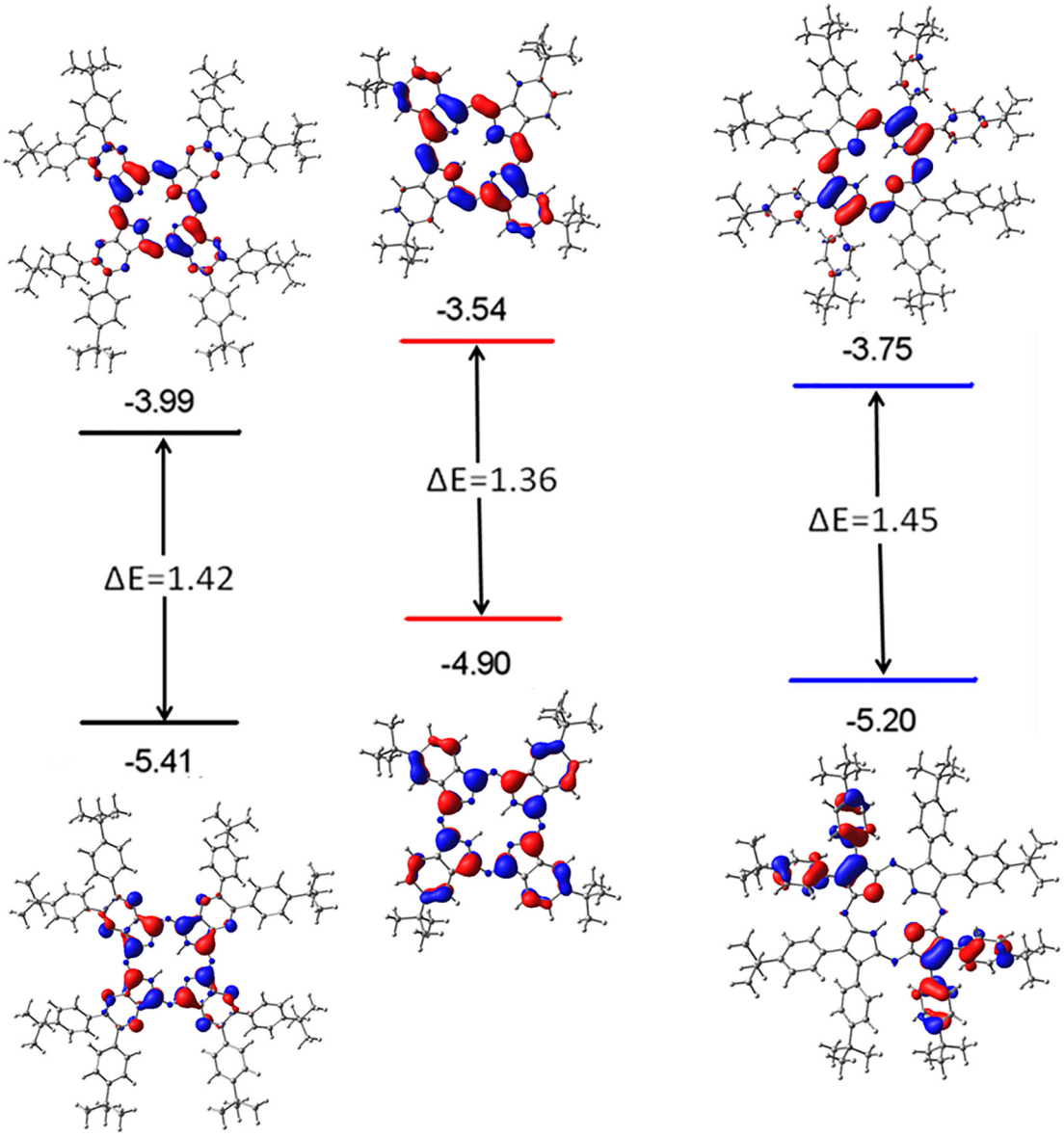

Fig. 6. The molecular orbitals energy (eV) of compounds (I-III).

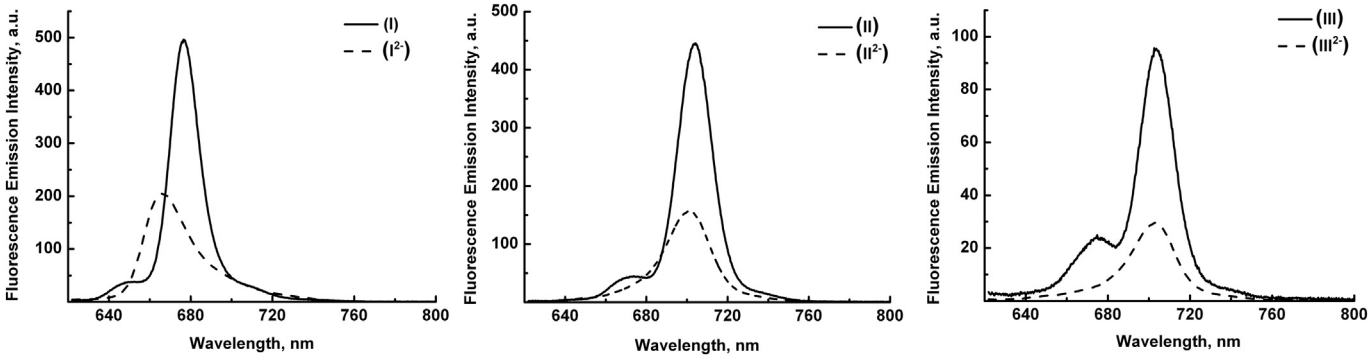

Fig. 7. Fluorescence spectra of the compounds (I-III) in acetonitrile and their deprotonated forms (I^{2-}, II^{2-}, III^{2-}) in an acetonitrile-DBU mixture at T = 295 K and λ_{ex} = 608 nm.

(III), which suggests a higher conformational mobility of the molecules in the first excited state in contrast to other compounds. As a result, a strong distortion of the conformation of compound (III) leads to an increase the rate of radiationless deactivation of the excited S_1 state and fluorescence quenching as evidenced by the low value of the quantum yield of fluorescence (Table 1). The presence of a complex system of substituents in the case of compound (I), where *tert*-butyl substituents of phenyl fragments are removed from the macrocyclic core (center of the macrocycle), than in ligand (II), leads to less fluorescence quenching (Table 1). Thus, the fluorescence quantum yield decreases in the following order: (I) > (II) > (III).

The hyperchromic shift is observed in the fluorescence spectra of deprotonated ligands compared to the free base of porphyrins (Fig. 7). This behavior is explained by the result of increased spin-orbit interaction, which leads to a more efficient intersystem transition from the lowest excited state of the singlet porphyrin S_1 to the corresponding triplet manifold [36] and thereby reduces the probability of fluorescence radiation and an increase in the viscosity of the solution.

Significantly large Δss values in the case of deprotonated porphyrins compared with free bases indicate a larger magnitude of structural rearrangements in the excited S_1 for compound II^{2-} and III^{2-}. The increase in macrocycle structure flexibility with a decrease in steric hindrance imposed leads to an increase in conformational mobility of the compounds in the first excited state S_1. Moreover, the deprotonated ligand (III^{2-}) has a greater conformational mobility due to the distortion of the macrocycle under the influence of eight *tert*-butyl substituents in the *para*-positions of the phenyl rings. The compound (I) in both deprotonated and molecular forms has a lower conformational dynamics. The conformational rigidity of macrocycle (I) is likely caused by steric hindrance with phenyl ligand.

The quantum fluorescence yields of the ionized forms of porphyrins decrease as a result of deprotonation of the macrocyclic nucleus, which leads to a greater distortion of the deprotonated ligand conformations (Fig. 5 and Table 1) and, as a result, an enhancement of the radiationless $S_1 \rightarrow S_0$ internal conversion rate [36,37] and quenching of fluorescence.

Table 1
Spectral-fluorescence characteristics of the compounds (I-III) in acetonitrile and their deprotonated forms (I^{2-}, II^{2-}, III^{2-}) in an acetonitrile-DBU mixture at T = 295 K and λ_{ex} = 608 nm.

Compound	λ_{fl} (nm)	Δ_{SS} (cm^{-1})	$Q_x \times 10^{-2}$
(**I**)	676.6	57.01	55.5
($\mathbf{I^{2-}}$)	665.6	31.6	4.8
(**II**)	704.2	105.6	21.0
($\mathbf{II^{2-}}$)	701.6	539.8	1.2
(**III**)	704.2	636.2	0.5
($\mathbf{III^{2-}}$)	703.6	668.3	0.1

4. Conclusions

Thus, in the present work, the synthesis and identification of tetrakis-[5,6-bis(4-*tert*-butylphenyl)pyrazino]porphyrazine, tetra-(4-*tert*-butyl) phthalocyanine and octakis-(4-*tert*-butylphenyl)porphyrazine were carried out. The spectrophotometric method was used to study the spectral, acidic and fluorescence properties of synthesized compounds. Geometry optimization and an analysis of the energy levels and localization of highest occupied and the lowest unoccupied molecular orbitals of the synthesized porphyrazines were performed on the basis of density functional theory with the BP86 functional and the def2-TZVP basis set. Given that the synthesized *tert*-butyl-substituted porphyrazines exhibit a high sensitivity of fluorescence to the molecule ionization they can be considered as promising materials for the design of sensors of the medium basicity. Research on the design of solid-state sensors based on them is running in the laboratory now.

Supplementary data to this article can be found online at https://doi.org/10.1016/j.saa.2020.118601.

Declaration of competing interest

We confirm the absence of a conflict of interest.

Acknowledgements

This work was supported by the Russian Science Foundation (Project number no. 19-73-20079, in the part of investigation of fluorescence properties and quantum-chemical modeling of the *tert*-butyl-substituted porphyrazines) and State Assignment for the Implementation of Scientific Research (Theme no. FZZW-2020-0008, in the part of synthesis of the *tert*-butyl-substituted porphyrazines).

The authors thank the Shared Facilities Center of the Institute of Organic Chemistry of the Russian Academy of Sciences for the equipment provided for the research and the Joint Supercomputer Center of the Russian Academy of Sciences (Moscow) for providing the resources of the MVS-100K cluster.

References

[1] M.S. Rodríguez-Morgade, P.A. Stuzhin, The chemistry of porphyrazines: an overview, J. Porphyrins Phthalocyanines 8 (2004) 1129–1165, https://doi.org/10.1142/S1088424604000490.

[2] K. Kopecky, V. Novakova, M. Miletin, R. Kučera, P. Zimcik, Synthesis of new azaphthalocyanine dark quencher and evaluation of its quenching efficiency with different fluorophores, Tetrahedron 67 (2011) 5956–5963, https://doi.org/10.1016/j.tet.2011.06.038.

[3] D.T. Mlynarczyk, J. Piskorz, L. Popenda, M. Stolarska, W. Szczolko, K. Konopka, S. Jurga, L. Sobotta, J. Mielcarek, N. Düzgüneş, T. Goslinski, S-seco-porphyrazine as a new member of theseco-porphyrazine family - synthesis, characterization and photocytotoxicity against cancer cells, Bioorg. Chem. 96 (2020) 103634, https://doi.org/10.1016/j.bioorg.2020.103634.

[4] E.R. Trivedi, B.J. Vesper, H. Weitman, B. Ehrenberg, A.G.M. Barrett, J.A. Rodasevich, B.M. Hoffman, Chiral bis-acetal porphyrazines as near-infrared optical agents for detection and treatment of cancer, Photochem. Photobiol. 86 (2010) 410–417, https://doi.org/10.1111/j.1751-1097.2009.00681.x.
[5] P.A. Tarakanov, A.O. Simakov, E.N. Tarakanova, A.V. Chernyak, V. Klykov, P.A. Stuzhin, V.E. Pushkarev, A sterically driven approach to the efficient synthesis of low-symmetry 1,4-diazepinoporphyrazines, Macroheterocycles 11 (2018) 312–315, https://doi.org/10.6060/mhc180484t.
[6] T. Venkataraman, Analytical Chemistry of Synthetic Dyes, J. Wiley, New York, 1977.
[7] S. Tomachynskyi, S. Korobko, L. Tomachynski, V. Pavlenko, Synthesis and spectral properties of new tetrakis-2,3-{5,7-bis[(E)-2-(4-methylphenyl)vinyl]pyrazino} porphyrazine metal complexes, Opt. Mater. 33 (2011) 1553–1556, https://doi.org/10.1016/j.optmat.2011.02.010.
[8] P. Petrik, P. Zimcik, K. Kopecky, Z. Musil, M. Miletin, V. Loukotova, Protonation and deprotonation of nitrogens in tetrapyrazino-porphyrazine macrocycles, J. Porphyrins Phthalocyanines 11 (2007) 487–495, https://doi.org/10.1142/S1088424607000564.
[9] Y.V. Karyakin, I.I. Angelov, Pure Chemical Reagents, Goskhimizdat, Moscow, 1955.
[10] Yu.B. Ivanova, Yu.I. Churakhina, N.Zh. Mamardashvili, Synthesis and basic properties of bisporphyrinocalix[4]arene, Russ. J. Gen. Chem. 78 (2008) 673–677, https://doi.org/10.1134/S1070363208040269.
[11] Yu.B. Ivanova, V.B. Sheinin, N.Zh. Mamardashvili, Porphyrin halide ion receptor, Russ. J. Gen. Chem. 77 (2007) 1458–1462, https://doi.org/10.1134/S1070363207080270.
[12] Yu.B. Ivanova, N.Zh. Mamardashvili, Fluorescent properties and kinetic rate constants of some Zn-tetraarylporphyrins formation in acetonitrile, J. Fluoresc. 27 (2017) 303–307, https://doi.org/10.1007/s10895-016-1958-1.
[13] S. Dhami, A.J. de Mello, G. Rumbles, S.M. Bishop, D. Phillips, A. Beeby, Phthalocyanine fluorescence at high concentration: dimers or reabsorption effect? Photochem. Photobiol. 61 (1995) 341–346, https://doi.org/10.1111/j.1751-1097.1995.tb08619.x.
[14] M. Whalley, 182. Conjugated macrocycles. Part XXXII. Absorption spectra of tetrazaporphins and phthalocyanines. Formation of pyridine salts, J. Chem. Soc. (1961) 866–869, https://doi.org/10.1039/JR9610000866.
[15] J.R. Lakowicz, Principles of Fluorescence Spectroscopy, Third edition Springer, University of Maryland School of Medicine Baltimore, Maryland, USA, 2010.
[16] M.W. Schmidt, K.K. Baldridge, J.A. Boatz, S.T. Elbert, M.S. Gordon, J.H. Jensen, S. Koseki, N. Matsunaga, K.A. Nguyen, S. Su, T.L. Windus, M. Dupuis, J.A. Montgomery, General atomic and molecular electronic structure system, J. Comput. Chem. 14 (1993) 1347–1363, https://doi.org/10.1002/jcc.540141112.
[17] A.D. Becke, Density-functional exchange-energy approximation with correct asymptotic behavior, Phys. Rev. A 38 (1988) 3098–3100, https://doi.org/10.1103/PhysRevA.38.3098.
[18] J.P. Perdew, Density-functional approximation for the correlation energy of the inhomogeneous electron gas, Phys. Rev. B 33 (1986) 8822–8824, https://doi.org/10.1103/PhysRevB.33.8822.
[19] A. Schaefer, H. Horn, R. Ahlrichs, Fully optimized contracted Gaussian basis sets for atoms Li to Kr, J. Chem. Phys. 97 (1992) 2571–2577, https://doi.org/10.1063/1.463096.
[20] H. Hirao, Which DFT functional performs well in the calculation of methylcobalamin? Comparison of the B3LYP and BP86 functionals and evaluation of the impact of empirical dispersion correction, J. Phys. Chem. A 115 (2011) 9308–9313, https://doi.org/10.1021/jp2052807.
[21] V.N. Nemykin, J.R. Sabin, Profiling energetics and spectroscopic signatures in prototropic tautomers of asymmetric phthalocyanine analogues, J. Phys. Chem. A 116 (2012) 7364–7371, https://doi.org/10.1021/jp304386x.
[22] C. Colomban, E.V. Kudrik, V. Briois, J.C. Shwarbrick, A.B. Sorokin, P. Afanasiev, X-ray absorption and emission spectroscopies of X-bridged diiron phthalocyanine complexes (FePc)2X (X = C, N, O) combined with DFT study of (FePc)2X and their high-valent diiron oxo complexes, Inorg. Chem. 53 (2014) 11517–11530, https://doi.org/10.1021/ic501463q.
[23] A.G. Martynov, J. Mack, A.K. May, T. Nyokong, Y.G. Gorbunova, A.Y. Tsivadze, Methodological survey of simplified TD-DFT methods for fast and accurate interpretation of UV–Vis–NIR spectra of phthalocyanines, ACS Omega 4 (2019) 7265–7284, https://doi.org/10.1021/acsomega.8b03500.
[24] J. Tomasi, M. Persico, Molecular interactions in solution: an overview of methods based on continuous distributions of the solvent, Chem. Rev. 94 (1994) 2027–2094, https://doi.org/10.1021/cr00031a013.
[25] S. Miertus˘, E. Scrocco, J. Tomasi, Electrostatic interaction of a solute with a continuum. A direct utilizaion of AB initio molecular potentials for the prevision of solvent effects, Chem. Phys. 55 (1981) 117–129, https://doi.org/10.1016/0301-0104(81)85090-2.
[26] R. Cammi, J. Tomasi, Remarks on the use of the apparent surface charges (ASC) methods in solvation problems: iterative versus matrix-inversion procedures and the renormalization of the apparent charges, J. Comput. Chem. 16 (1995) 1449–1458, https://doi.org/10.1002/jcc.540161202.
[27] W. Freyer, Octa-(4-*tert*-butylphenyl)-tetrapyrazinoporphyrazina end its metal complexes, J. Prakt. Chem. 336 (1994) 690–692.
[28] R. Li, X. Zhang, P. Zhu, D.K.P. Ng, N. Kobayashi, J. Jiang, Electron-donating or -withdrawing nature of substituents revealed by the electrochemistry of metal-free phthalocyanines, Inorg. Chem. 45 (2006) 2327–2334, https://doi.org/10.1021/ic051931k.
[29] E.E. Joslin, J.P.T. Zaragoza, R.A. Baglia, M.A. Siegler, D.P. Goldberg, The influence of peripheral substituent modification on P^{V}, Mn^{III}, and Mn^{V} (O) corrolazines: X-ray crystallography, electrochemical and spectroscopic properties, and HAT and OAT reactivities, Inorg. Chem. 55 (2016) 8646–8660, https://doi.org/10.1021/acs.inorgchem.6b01219.
[30] V.B. Sheinin, Yu.B. Ivanova, The acid properties of benzodiamyloxyl and thiadiazole porphyrazine derivatives in the H 2 L-(K [2.2. 2]) OH-DMSO system, Russ. Journ. Phys. Chem. A 81 (2007) 1250–1255, https://doi.org/10.1134/S0036024407080134.
[31] O.A. Petrov, G.V. Osipova, O.G. Khelevina, Reactivity of porphyrazines in acid-base interaction with N-bases, Macroheterocycles 2 (2009) 151–156, https://doi.org/10.6060/mhc2009.2.151.
[32] I. Ya, Bernstein, Spectrophotometric Analysis in Organic Chemistry. M: Chemistry, 1986 (in Russ.).
[33] V.G. Andrianov, O.V. Malkova, Acid-base properties of porphyrins in nonaqueous solutions, Macroheterocycles 2 (2009) 130–138, https://doi.org/10.6060/mhc2009.2.130.
[34] I. Fleming, Frontier Orbitals and Organic Chemical Reactions, Wiley, London, 1976.
[35] W. Freyer, S. Mueller, K.J. Teuchner, Photophysical properties of benzoannelated metal-free phthalocyanines, Photochem. Photobiol. A Chem. 163 (2004) 231–240, https://doi.org/10.1016/j.jphotochem.2003.12.003.
[36] G. De Luca, A. Romeo, L.M. Scolaro, G. Ricciardi, A. Rosa, Evidence for tetraphenylporphyrin monoacids, Inorg. Chem. 46 (2007) 5979–5988, https://doi.org/10.1021/ic0703373.
[37] I.V. Vershilovskaya, S. Stefani, P. Verstappen, T.H. Ngo, I.G. Scheblykin, W. Dehaen, W. Maes, M.M. Kruk, Spectral-luminescent properties of meso-tetraarylporphyrins revisited: the role of aryl type, substitution pattern and macrocycle core protonation, Macroheterocycles 10 (2017) 257–267, https://doi.org/10.6060/mhc160962n.